AIP | Applied Physics Letters

Predicting the closed-loop stability and oscillation amplitude of nonlinear parametrically amplified oscillators

V. Zega, S. Nitzan, M. Li, C. H. Ahn, E. Ng, V. Hong, Y. Yang, T. Kenny, A. Corigliano, and D. A. Horsley

Citation: Applied Physics Letters **106**, 233111 (2015); doi: 10.1063/1.4922533
View online: http://dx.doi.org/10.1063/1.4922533
View Table of Contents: http://scitation.aip.org/content/aip/journal/apl/106/23?ver=pdfcov
Published by the AIP Publishing

Predicting the closed-loop stability and oscillation amplitude of nonlinear parametrically amplified oscillators

V. Zega,[1,a)] S. Nitzan,[2] M. Li,[3] C. H. Ahn,[4] E. Ng,[4] V. Hong,[4] Y. Yang,[4] T. Kenny,[4] A. Corigliano,[1] and D. A. Horsley[2,b)]
[1]*Civil and Environmental Engineering, Politecnico di Milano, 20133 Milan, Italy*
[2]*Mechanical and Aerospace Engineering, University of California, Davis, Davis, California 95616, USA*
[3]*Electrical and Computer Engineering, University of California, Davis, Davis, California 95616, USA*
[4]*Mechanical Engineering, Stanford University, Stanford, California 94305, USA*

(Received 2 February 2015; accepted 3 June 2015; published online 11 June 2015)

This work investigates the closed-loop operation of microelectromechanical oscillators in the presence of both cubic (Duffing) nonlinearities and parametric amplification. We present a theoretical model for this system that enables us to predict oscillation amplitude and instability and experimentally verify it using a silicon disk resonator with a quality factor (Q) of 85 000 and a natural frequency of 251 kHz. We determine that, contrary to previous understanding gained from analyzing the open-loop system, the presence of cubic nonlinearities does not limit the maximum stable oscillation amplitude if the resonator is operated in a closed loop. In addition, the stability and amplitude behavior predicted by our theoretical model are independent of the presence or severity of cubic nonlinearities, or on drive amplitude. © *2015 AIP Publishing LLC*.
[http://dx.doi.org/10.1063/1.4922533]

Micromechanical resonators are widely used in many applications, such as oscillators for timekeeping[1] and gyroscopes,[2–6] where large oscillation amplitude is desirable as it increases the signal level, improving signal to noise ratio in gyroscopes and reducing phase noise in oscillators. However, at large amplitudes, these micro- and nano-scale resonators begin to exhibit nonlinearities such as the Duffing oscillator behavior that arises from cubic stiffness nonlinearity. Because the nonlinear threshold scales with resonator size, this has long been viewed as a limitation on the ultimate size of such resonators, since nonlinear behavior has been associated with degraded performance in open loop devices.[7] However, closed-loop devices exhibit different dynamics, and it has been shown that Duffing behavior does not pose a problem for stable closed-loop operation of micromechanical oscillators[8] and gyroscopes,[9] and there is growing interest in exploiting this and other nonlinearities[10–15] to improve device performance. Parametric resonance is one such nonlinear amplification method. Recently, parametric resonance was observed to arise from nonlinear mechanical stiffness coupling between the degenerate vibration modes of a high quality-factor silicon disk resonator used as a gyroscope.[16] The device's exceptionally high quality factor ($Q = 85\,000$) was shown to result in a high degree of sensitivity to small mechanical nonlinearities resulting from stress concentrations, ultimately causing the device to exhibit both the classical Duffing oscillator behavior as well as the newly observed parametric resonance. This combination of Duffing and parametric nonlinearities can also occur when parametric amplification is used to actuate the drive or sense axis of a gyroscope[3–5,17–19] and has implications for timing applications[1] as well. For devices such as these gyroscopes and oscillators, which, either due to high Q or due to small resonator size, exhibit nonlinearity at small displacements, a theoretical model of closed-loop operation in the presence of these nonlinearities is needed to enable operation at large amplitudes and to inform decisions regarding the design and operation of these resonators. While the established approach is to design the resonator structure and control loop to avoid nonlinear operation, better understanding of the benefits and penalties of nonlinear operation could vastly improve device performance through either increased signal levels (through larger amplitude oscillation) or reduced device size.

Open-loop, parametrically amplified Duffing oscillators have been studied,[20–26] and their corresponding stability limits are well-understood. In Ref. 27, Rhoads and Shaw use the method of averaging to compute theoretical steady-state responses for a parametrically amplified Duffing oscillator operating in open loop and present the resulting amplitude-frequency and phase-frequency curves. They conclude that stable open-loop operation is possible, but only at the cost of decreased performance or bistable behavior. Here, in addition to the analysis presented by Rhoads and Shaw, we examine the closed-loop behavior of this system. We extend their analysis, using the same steady-state solution, but examining the amplitude-phase relationship of the steady-state solutions, a technique which is useful for predicting the closed-loop behavior of nonlinear oscillators.[8,9,28,29] We show that for closed-loop oscillators, stable, parametrically amplified operation in the presence of cubic nonlinearities is possible without suffering from jump instabilities, hysteresis, or degraded performance. The resulting analysis is shown to predict the experimentally observed behavior of the high-Q silicon disk resonator.

In order to determine the closed-loop behavior of a parametrically amplified Duffing oscillator, the modified Mathieu equation

[a)]This research was performed while V. Zega was at University of California, Davis, Davis, California 95616, USA.
[b)]Author to whom correspondence should be addressed. Electronic mail: dahorsley@ucdavis.edu.

$$\ddot{x} + \frac{\omega}{Q}\dot{x} + \left[1 + \frac{\Delta k}{k}\cos(2\omega t) + \frac{k_3}{k}x^2\right]\omega^2 x = \frac{F}{m}\cos(\omega t + \phi) \tag{1}$$

must be analyzed. Here, x is the displacement, m is the modal mass,[30] ω is the resonant frequency, Q is the quality factor, k is the stiffness, $\frac{\Delta k}{k} = \lambda$ is the parametric pump input (normalized stiffness change of the resonator occurring at frequency 2ω), k_3 is the cubic nonlinearity, and $F\cos(\omega t + \phi)$ is the harmonic drive force applied at ω. If $k_3 = 0$, Eq. (1) describes a degenerate parametric amplifier and the motion resulting from F is either amplified or suppressed, depending on the phase, ϕ, of the applied 2ω pump relative to F. The total force-to-displacement gain at resonance is $G(\phi)Q/k$, where the phase-dependent parametric gain is given by[31]

$$G(\phi) = \left[\left(\frac{\cos(\phi)}{1 + \frac{Q\Delta k}{2k}}\right)^2 + \left(\frac{\sin(\phi)}{1 - \frac{Q\Delta k}{2k}}\right)^2\right]^{1/2}. \tag{2}$$

This function has a singularity at $\lambda_c = 2/Q$, which results in autoparametric oscillation at frequency 1ω for $\lambda > \lambda_c$. Once cubic nonlinearity is included ($k_3 \neq 0$), Eq. (1) has no closed-form solution; however, Rhoads and Shaw compute the system response by nondimensionalizing Eq. (1) and applying perturbation methods, specifically, by the method of averaging.[27] Although this approximate solution is closed-form, it is non-trivial. This method was used to solve for the response of a highly nonlinear system ($\frac{k_3}{k} = -2 \times 10^{10}$) operated close to the autoparametric limit ($\lambda/\lambda_c = 0.95$) with a pump phase of $\phi = 90°$. The magnitude and phase frequency responses, Fig. 1(a), are multivalued at large amplitude and are strongly dependent on the value of the cubic term, k_3, consistent with Rhoads' and Shaw's result. Here, k_3 is negative, but for positive values of k_3 the amplitude-frequency response will bend instead to the right. However, the amplitude-phase plot of the same model, Fig. 1(b), is single valued and the same plot is obtained regardless of the value or sign of k_3, making this a useful tool for subsequent analysis. Note that in Fig. 1, the amplitude of the response is normalized to the linear response that would be obtained in the absence of parametric amplification and cubic nonlinearity, and the frequency is presented in non-dimensionalized form, $\sigma = \omega t/Q$. For a closed-loop system θ, the phase shift across the resonator can be experimentally varied by using a phase-locked loop (PLL), so that the closed-loop oscillation is forced to take place at a given phase, rather than a given frequency, as will be discussed in detail below.

The amplitude-phase plots of parametrically amplified Duffing oscillators are shown for varying pump phase, ϕ, and pump amplitude, λ, in Fig. 2. In this investigation, we use the numerical values for the system parameters shown in Table I, which correspond to the parameters of the resonator used in experiments described below. At pump amplitudes above λ_c, the solution becomes unstable for a range of phases, as indicated by the dashed lines, and autoparametric excitation ensues.[5,31] In practice, the maximum amplitude of the system will be limited by other nonlinearities[32] or mechanical contact between the resonator and its surroundings.

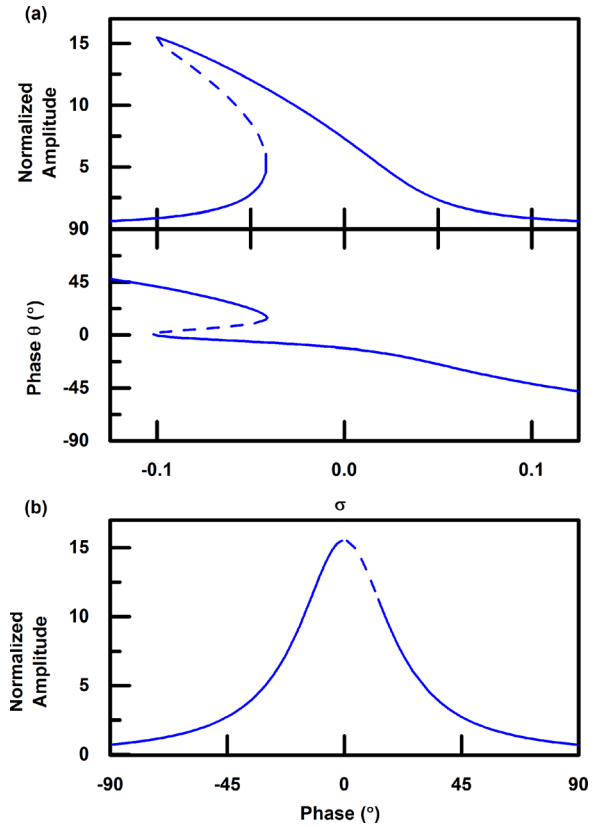

FIG. 1. Steady-state response of a highly nonlinear system ($\frac{k_3}{k} = -2 \times 10^{10}$) with a large-amplitude parametric pump ($\lambda/\lambda_c = 0.95$) operated with a pump phase $\phi = 90°$. Dashed lines indicate solutions which are unstable in the open loop. (a) Normalized amplitude and phase versus non-dimensionalized frequency ($\sigma = \omega t/Q$). The frequency response is multi-valued. (b) Response of the same system plotted as normalized amplitude versus phase. The amplitude-phase response is single-valued and is used to predict closed-loop behavior.

In order to experimentally verify these results, we used a high-Q single-crystal silicon disk resonator originally presented in Refs. 33 and 34. This 600 μm diameter device is encapsulated at a low pressure (1 Pa) by an epitaxial silicon layer in order to achieve high Q (85 000). The epi-seal encapsulation process was proposed by researchers at the Robert Bosch Research and Technology Center in Palo Alto and then demonstrated in a close collaboration with Stanford University. This collaboration is continuing to develop improvements and extensions to this process for many applications, while the baseline process has been brought into commercial production by SiTime, Inc. The disk resonator used here, shown in Fig. 3, supports two degenerate elliptical modes at 251 kHz, as well as higher-order modes both in-plane and out-of-plane. Because the two degenerate elliptical modes are flexurally coupled, stress concentrations resulting from the displacement of one mode can modulate the stiffness of the orthogonal mode, resulting in parametric amplification.[16] Here, we use one of the two degenerate elliptical modes and electrostatically tune the second mode to a different resonant frequency to prevent modal coupling from perturbing the results. Higher order modes are not integer multiples of the elliptical mode's resonant frequency and hence are not of concern. The system parameters are presented in Table I.

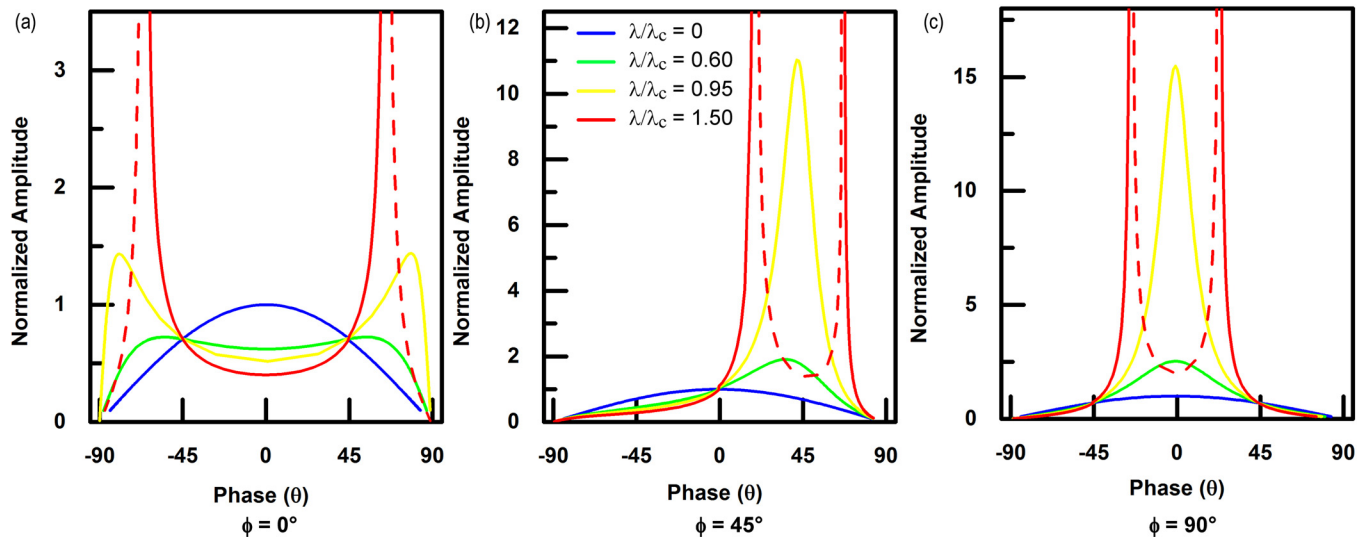

FIG. 2. Amplitude-phase plots for an oscillator following the nonlinear Mathieu equation presented in Eq. (1) above. System parameters are given in Table I. The result varies depending on the phase shift, ϕ, between the 1 ω excitation and the 2ω pump, and the results are plotted for (a) $\phi = 0°$, (b) $\phi = 45°$, and (c) $\phi = 90°$. Above the threshold for autoparametric excitation, the solution becomes unstable, as indicated by dashed lines.

TABLE I. Resonator parameters.

Parameter	Value
$f_n = \omega/2\pi$	251 kHz
Q	85 000
m	3.9 μg
k	9970 N/m
k_3	-1.99×10^{13} N/m^3

A block diagram of the test system is shown in Fig. 4. The resonator is locked into closed-loop oscillation with constant amplitude using a digital PLL. While in a conventional oscillator, Barkhausen's criterion states that oscillation occurs at the frequency where the phase shift around the loop θ is equal to zero; the PLL allows the phase shift to be adjusted to an arbitrary value. A second electrostatic input at twice the forcing frequency (2ω) is then used to modulate the stiffness of the structure. Details on electrostatic stiffness modulation can be found in Refs. 30 and 35. A phase shift, ϕ, is introduced between the 1ω and 2ω signals to study the phase-dependent parametric gain.

The experimental amplitude-phase curves are collected for $\phi = 0°$, 45°, and 90°, and for $\lambda/\lambda_c = 0$, 0.34, and 0.64. The results are then normalized to the peak amplitude obtained when $\lambda/\lambda_c = 0$, and superposed with the theoretical prediction, as shown in Fig. 5. The experimental results agree very well with theory. Notice that, in comparison to a classical linear oscillator, where maximum amplitude occurs at 0° phase shift around the loop and the amplitude-phase plot is symmetric about this point, in the parametric oscillator, the phase shift resulting in maximum amplitude is dependent on the phase of the applied parametric pump, ϕ, and the amplitude-phase curve is not symmetrical for some values of ϕ. Below the threshold for parametric instability, $\lambda/\lambda_c = 1$, the amplitude-phase curve is finite, with the maximum amplitude occurring at a phase θ that depends on the phase shift, ϕ, between the 1ω excitation and 2ω parametric pump. System behavior is dependent on whether the system is operated at resonance ($\theta = 0$) or at a frequency (and therefore a phase) offset. When $\phi = 0°$ (Figures 2 and 5(a)), operation at $\theta = 0$ results in suppressed output for increasing

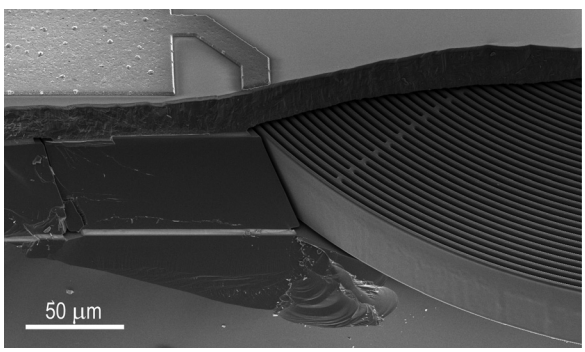

FIG. 3. Scanning electron microscope (SEM) image showing the disk resonator. The device is encapsulated at a low pressure (1 Pa) resulting in high Q and supports two elliptical modes at 251 kHz, as well as higher-order modes both in plane and out of plane.

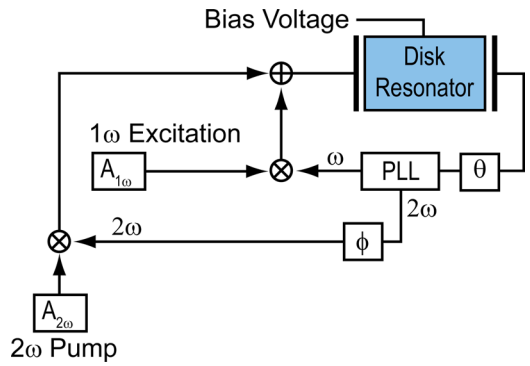

FIG. 4. Block diagram of the closed-loop oscillator control system. Excitation at 1ω is produced by the PLL which enables the phase shift around the loop, θ, to be varied arbitrarily while a secondary 2ω pump input is used to parametrically amplify this excitation. The relative phase, ϕ, between the 1ω PLL output and $2\,\omega$ pump can be varied.

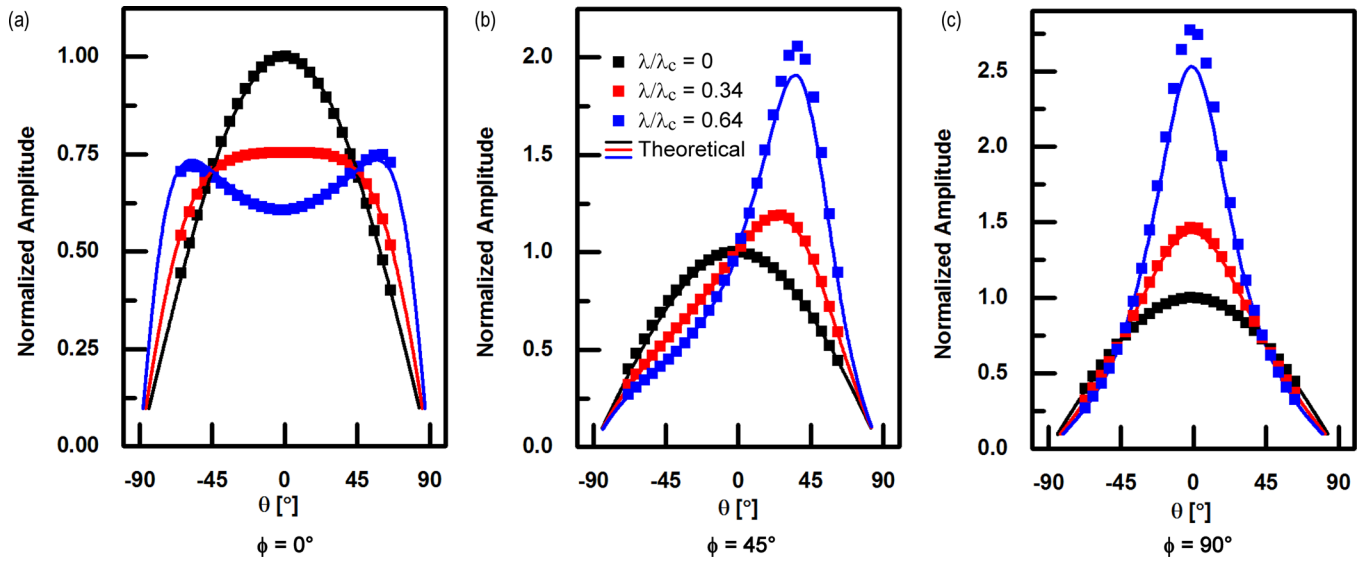

FIG. 5. Experimentally measured amplitude-phase plots, with the 2ω pump applied at three values of relative phase, ϕ. The amplitude is normalized to the $\lambda = 0$ (linear oscillator) case. Theoretical predictions (superposed) are in close agreement with experimental results.

pump amplitudes; however, off-resonant excitation can result in amplification. When $\phi = 45°$ (Figures 2 and 5(b)), no amplification is present for $\theta = 0$, and phase offsets in each direction result in either amplification or suppression of input signals, dependent on the direction of the offset. For $\phi = 90°$ (Figures 2 and 5(c)), operation at $\theta = 0$ results in finite amplification, provided $\lambda < \lambda_c$. Above λ_c, autoparametric excitation is possible regardless of ϕ; however, the phase shift required to produce an unstable (autoparametric) response varies with the relative phase of the pump input. It would be possible, for instance, to achieve autoparametric excitation with a pump phase of $\phi = 0°$, an angle ordinarily associated with suppression, if the oscillator loop locks to $\theta = \pm 90°$ (off-resonance).

From the above analysis, we can conclude that stable closed-loop parametric amplification in the presence of Duffing nonlinearities is possible, and we can predict that the behavior of the system as the phase shift around the loop and relative phase of the pump input are varied. In particular, the amplitude-phase dependence presented in Fig. 2 can be used to predict the behavior of parametrically amplified systems operating in a closed loop with arbitrary cubic nonlinearity k_3. In addition, we note that the closed-loop oscillation amplitude is independent of k_3 and scales linearly with drive force for any given pump phase shift and amplitude, provided $\lambda < \lambda_c$. Thus, the oscillation amplitude is not inherently limited by nonlinearity k_3, as was previously understood. We also experimentally verify the theoretical results presented in Fig. 2 and demonstrate that the model can be used to predict the stable closed-loop oscillation amplitude of a parametrically amplified Duffing oscillator for a variety of pump amplitudes and phase shifts.

This project was funded by DARPA under Contract Nos. W31P4Q-12-1-0001 and N66001-12-1-4260. The device was fabricated at the Stanford Nanofabrication Facility. Valentina Zega thanks STMicroelectronics for her Ph.D. grant, and Professor D. Horsley and the whole group of BSAC at UCD for kind hospitality.

[1]L. G. Villanueva, R. B. Karabalin, M. H. Matheny, E. Kenig, M. C. Cross, and M. L. Roukes, Nano Lett. **11**(11), 5054 (2011).
[2]C. Ahn, S. Nitzan, E. Ng, V. Hong, Y. Yang, T. Kimbrell, D. A. Horsley, and T. Kenny, Appl. Phys. Lett. **105**, 243504 (2014).
[3]M. Sharma, E. H. Sarraf, R. Baskaran, and E. Cretu, Sens. Actuators, A **177**, 79 (2012).
[4]B. J. Gallacher and J. S. Burdess, Proc. Inst. Mech. Eng., Part C **220**(9), 1463 (2006).
[5]B. J. Gallacher, J. S. Burdess, and K. M. Harish, J. Micromech. Microeng. **16**(2), 320 (2006).
[6]W. Zhang, R. Baskaran, and K. Turner, Appl. Phys. Lett. **82**(1), 130 (2003).
[7]V. Kaajakari, T. Mattila, A. Oja, and H. Seppa, J. Microelectromech. Syst. **13**(5), 715 (2004).
[8]L. Hyung Kyu, R. Melamud, S. Chandorkar, J. Salvia, S. Yoneoka, and T. W. Kenny, J. Microelectromech. Syst. **20**(6), 1228 (2011).
[9]S. Nitzan, T. H. Su, C. Ahn, E. Ng, V. Hong, Y. Yang, T. Kenny, and D. A. Horsley, paper presented at the IEEE 27th International Conference on Micro Electro Mechanical Systems (MEMS), 2014.
[10]R. Almog, S. Zaitsev, O. Shtempluck, and E. Buks, Appl. Phys. Lett. **88**(21), 213509 (2006).
[11]L. G. Villanueva, E. Kenig, R. B. Karabalin, M. H. Matheny, R. Lifshitz, M. C. Cross, and M. L. Roukes, Phys. Rev. Lett. **110**(17), 177208 (2013).
[12]D. S. Greywall, B. Yurke, P. A. Busch, A. N. Pargellis, and R. L. Willett, Phys. Rev. Lett. **72**(19), 2992 (1994).
[13]B. Yurke, D. Greywall, A. Pargellis, and P. Busch, Phys. Rev. A **51**(5), 4211 (1995).
[14]Y. Yang, E. Ng, V. Hong, C. Ahn, Y. Chen, E. Ahadi, M. Dykman, and T. Kenny, "Measurement of the Nonlinearity of Doped Bulk-Mode MEMS Resonators," presented at the Solid-State Sensors, Actuators, and Microsystems Workshop, Hilton Head Island, SC, USA, 8–12 June 2014, pp. 285–288.
[15]J. Nichol, E. Hemesath, L. J. Lauhon, and R. Budakian, Appl. Phys. Lett. **95**, 123116 (2009).
[16]S. Nitzan, V. Zega, M. Li, C. H. Ahn, A. Corigliano, and D. A. Horsley, Sci. Rep. **5**, 9036 (2015).
[17]M. Sharma, E. H. Sarraf, and E. Cretu, paper presented at the IEEE 24th International Conference on Micro Electro Mechanical Systems (MEMS), 2011.
[18]L. A. Oropeza-Ramos, C. B. Burgner, and K. L. Turner, Sens. Actuators, A **152**(1), 80 (2009).
[19]N. J. Miller, S. W. Shaw, L. A. Oropeza-Ramos, and K. L. Turner, in *ASME 2008 9th Biennial Conference on Engineering Systems and Analysis*, Haifa, Israel (2008), Vol. 2, p. 793.
[20]W. Zhang, R. Baskaran, and K. L. Turner, Sens. Actuators, A **102**(1–2), 139 (2002).
[21]M. V. Requa and K. L. Turner, Appl. Phys. Lett. **88**(26), 263508 (2006).
[22]Z. Wenhua, R. Baskaran, and K. L. Turner, paper presented at the IEEE 16th Annual International Conference on Micro Electro Mechanical Systems, MEMS-03, Kyoto, 2003.

[23]Z. Wen-Ming and M. Guang, IEEE Sens. J. **7**(3), 370 (2007).
[24]J. F. Rhoads, S. W. Shaw, K. L. Turner, J. Moehlis, B. E. DeMartini, and W. Zhang, J. Sound Vib. **296**(4–5), 797 (2006).
[25]W. Zhang and K. L. Turner, Sens. Actuators, A **122**(1), 23 (2005).
[26]R. Almog, S. Zaitsev, O. Shtempluck, and E. Buks, Phys. Rev. Lett. **98**(7), 078103 (2007).
[27]J. F. Rhoads and S. W. Shaw, Appl. Phys. Lett. **96**(23), 234101 (2010).
[28]J. Juillard, A. Bonnoit, E. Avignon, S. Hentz, N. Kacem, and E. Colinet, paper presented at the IEEE Sensors, 2008.
[29]C. Guo and G. K. Fedder, Appl. Phys. Lett. **103**(18), 183512 (2013).
[30]S. Tsanh-Hung, S. H. Nitzan, P. Taheri-Tehrani, M. H. Kline, B. E. Boser, and D. A. Horsley, IEEE Sens. J. **14**(10), 3426 (2014).
[31]D. Rugar and P. Grütter, Phys. Rev. Lett. **67**(6), 699 (1991).
[32]C. van der Avoort, R. van der Hout, J. J. M. Bontemps, P. G. Steeneken, K. Le Phan, R. H. B. Fey, J. Hulshof, and J. T. M. van Beek, J. Micromech. Microeng. **20**(10), 105012 (2010).
[33]S. Nitzan, C. H. Ahn, T. H. Su, M. Li, E. J. Ng, S. Wang, Z. M. Yang, G. O'Brien, B. E. Boser, T. W. Kenny, and D. A. Horsley, paper presented at the IEEE 26th International Conference on Micro Electro Mechanical Systems (MEMS), 2013.
[34]C. H. Ahn, E. J. Ng, V. A. Hong, Y. Yang, B. J. Lee, I. Flader, and T. W. Kenny, J. Micromech. Syst. **24**(2), 343 (2015).
[35]B. J. Gallacher, J. Hedley, J. S. Burdess, A. J. Harris, A. Rickard, and D. O. King, J. Microelectromech. Syst. **14**(2), 221 (2005).